



State-space analysis and identification for a class of hysteretic systems[☆]

Reinder Banning^{a,*}, Willem L. de Koning^b, Han J.M.T.A. Adriaens^c,
Richard K. Koops^d

^aSignals, Systems and Control Group, Department of Applied Physics, Delft University of Technology, Lorentzweg 1, 2628 CJ Delft, Netherlands

^bMathematical System Theory Group, Department of Information Technology and Systems, Delft University of Technology, 2628 CD Delft, Netherlands

^cASM Lithography, 5500 AH Veldhoven, Netherlands, formerly Mathematical System Theory Group, Department of Information Technology and Systems, Delft University of Technology, 2628 CD Delft, Netherlands

^dNMI-Institute for Metrology and Technology, Schoemakerstraat 97, 2628 VK Delft, Netherlands, formerly Delft Institute of Microelectronics and Submicrontechnology, Department of Applied Physics, Delft University of Technology, 2628 CD Delft, Netherlands

Received 21 July 1998; revised 22 March 2001; received in final form 15 May 2001

An identification technique is presented for certain non-linear state-space models describing systems under the influence of hysteresis

Abstract

In this paper we present results on the twin subjects of system analysis and system identification for a class of state-space realizable dynamic systems under the influence of hysteresis. The class of systems in question consists of models in the form of a linear time-invariant dynamic system in series with a differential model of hysteresis. It will be demonstrated that under fairly light constraints on the differential model of hysteresis, it is possible to design a series of experiments leading towards the identification of the full state-space realization. The approach is tested successfully on a high-precision mechanical translation system affected by hysteresis. © 2001 Elsevier Science Ltd. All rights reserved.

Keywords: Hysteresis loops; Non-linear systems; State-space models; Dynamic systems; System identification

1. Introduction

The word *hysteresis* originates from ancient Greek and means ‘to lag behind’. In mathematical terms, a hysteresis system is a dynamic system with an output variable that is invariant with respect to changes of the time scale (Visintin, 1994). Put differently, the hysteresis effect is the so-called *rate independent* or *persistent* and *scale-invariant* dynamic effect. Some of the best known examples of

hysteresis affected phenomena are to be found in plasticity, friction, ferromagnetism, and piezoelectricity (Coleman & Hodgdon, 1986; Holman, Laman, Scholte, Heerens, & Tuinstra, 1996; Krasnoselskii & Pokrovskii, 1989; Visintin, 1994). Consequently, it is not a surprise to learn that a composite mechanical/ferromagnetic/piezoelectric system is affected by hysteresis. Typically, such a system’s predominantly linear dynamic behaviour is infused with hysteresis.

The fact that hysteresis phenomena occur in a wide variety of areas has probably been the main obstacle on the road towards the development of a standard hysteresis model. As a consequence, a range of models is available (Krasnoselskii & Pokrovskii, 1989; Visintin, 1994), and each has been developed within the context of its own application. One of those hysteresis description formats, a first order scalar time-domain differential equation, stands out. It stands out because it suits our goal of

[☆]This paper was not presented at any IFAC meeting. This paper was recommended for publication in revised form by Editor Mituhiko Araki.

*Corresponding author. Tel.: +31-15-2785150; fax: +31-15-2784263.

E-mail addresses: r.banning@tn.tudelft.nl (R. Banning), w.l.dekoning@twi.tudelft.nl (W. L. de Koning), han.adriaens@asml.nl (H. J. M. T. A. Adriaens), rkoops@nmi.nl (R. K. Koops).

obtaining a dynamic model for a hysteretic system that is realizable in state-space. Ultimately, this model is used for the purpose of model-based feedback control. Although recent studies (Tao & Kokotovic, 1996; Ge & Jouaneh, 1996; Goldfarb & Celanovic, 1997) have demonstrated that description formats not in this form can be used successfully for control purposes, our preference goes to the aforementioned *differential model of hysteresis*.

A model with linear and hysteretic dynamic characteristics is obtained through the assignment of the output of a single-input/single-output linear dynamic system as the input of a single-input/single-output differential model of hysteresis. The overall dynamic model thus obtained, is readily realized in state-space. Subsequent work has demonstrated that it is possible to successfully design and implement tracking controllers on the basis of this state-space realization (Adriaens, de Koning, & Banning, 1999; Banning, de Koning, & Adriaens, 1999).

The organization of the paper is as follows. In Section 2, we present the individual models for hysteretic and linear dynamic behaviour. Subsequently, the overall model is constructed in the manner described above and an equivalent non-linear state-space representation is derived. The next section, Section 3, is devoted to the subject of system analysis. Note that not a complete analysis of the system’s dynamic behaviour is given. Indeed, only those aspects that have proved themselves useful for identification purposes, are presented. In Section 4, a set of tools for the complete identification of the state-space equivalent of the overall system dynamics is derived. In Section 5, the results of our modelling and identification efforts are tested on a high-precision translation stage with integrated sensors and actuators. The conclusions are presented in Section 6.

2. System definition

Let the matrix triplet (A_L, B_L, C_L) represent a state-space realization for a linear time-invariant single-input/single-output dynamic system, i.e. $(x_L(t_0) = x_{L,0} \in \mathbb{R}^{n-1}, u \in \mathbb{R}$ and $y_L \in \mathbb{R})$:

$$\Sigma_L \triangleq \begin{cases} \frac{dx_L(t)}{dt} = A_L x_L(t) + B_L u(t), \\ y_L(t) = C_L x_L(t). \end{cases} \quad (1)$$

By assumption, the unforced linear system is asymptotically stable, i.e. $\text{Re}[\lambda_i(A_L)] < 0$. Also, this system is considered to be a *minimum phase* system. Finally, the system is assumed to be such that in equilibrium, its output equals its input, i.e. $\bar{y}_L = \bar{u}$.

From a historical perspective, the differential model of hysteresis has been developed in the wider context of the theory of ferromagnetism (Krasnoselskii & Pokrovskii,

1989; Visintin, 1994; Coleman & Hodgdon, 1986). Mathematically speaking, the differential model of hysteresis is a representation of a rate independent dynamic effect in the form of a differential equation in the time domain. In this paper we take the latter, mathematical point of view, and adopt the following scalar differential model of hysteresis (Krasnoselskii & Pokrovskii, 1989; Visintin, 1994) as our *generic* model for hysteresis effects ($w(t_0) = w_0 \in \mathbb{R}, v(t) \in \mathbb{R}$):

$$\Sigma_H \triangleq \left\{ \frac{dw(t)}{dt} = h(v(t), \dot{v}(t), w(t)) \right. \quad (2)$$

with

$$h(v(t), \dot{v}(t), w(t)) = f(v(t), w(t))|\dot{v}(t)| + g(v(t), w(t))\dot{v}(t).$$

In the context of this paper, i.e. the state-space analysis and identification for the purpose of control, we only admit differential models of hysteresis based on a function $f(v(t), w(t))$ that is affine in $w(t)$, and a function $g(v(t), w(t))$ that is constant in $w(t)$. The resulting system function of the hysteresis model Σ_H is then equal to

$$h(v(t), \dot{v}(t), w(t)) = -\alpha w(t)|\dot{v}(t)| + \alpha|\dot{v}(t)|f(v(t)) + \dot{v}(t)g(v(t)) \quad (3)$$

with $0 < \alpha \in \mathbb{R}$. Model Σ_H with this system function has been used to characterize physical hysteresis phenomena, provided functions $f(\cdot)$ and $g(\cdot)$ comply with (Coleman & Hodgdon, 1986; Hodgdon, 1988):

- (1) real-valued function $f(\cdot)$ is odd, monotone increasing and piece-wise continuously differentiable with a finite limit for its first order derivative at positive infinity;
- (2) real-valued function $g(\cdot)$ is even, piece-wise continuous and at infinity of such a finite value that

$$\lim_{s \rightarrow +\infty} \frac{df(s)}{ds} = \lim_{s \rightarrow +\infty} g(s);$$

- (3) real-valued functions $f(\cdot)$ and $g(\cdot)$ are such that

$$g(s) \leq \frac{df(s)}{ds} \quad \forall s < \infty \quad (4)$$

and

$$\alpha e^{zs} \int_s^\infty \left[\frac{df(\zeta)}{d\zeta} - g(\zeta) \right] e^{-z\zeta} d\zeta \leq g(s) \quad \forall s < \infty. \quad (5)$$

It will be assumed from hereon that functions $f(\cdot)$ and $g(\cdot)$ comply with above conditions. The effects of inequalities (4) and (5) on the system’s behaviour is commented upon in detail in Section 3.2.

The overall dynamic model is constructed from systems Σ_L and Σ_H by applying the output of system Σ_L as the input to system Σ_H . For the resulting system, the

following state-space realization can be formulated ($x_0 = [x_{L,0}^T \ w_0^T]^T \in \mathbb{R}^n$):

$$\Sigma_0 \triangleq \begin{cases} \frac{dx(t)}{dt} = Ax(t) + H(x(t), u(t)), \\ y(t) = Cx(t) \end{cases} \quad (6)$$

with

$$A = \begin{bmatrix} A_L & 0 \\ 0 & 0 \end{bmatrix}, \quad C = [0 \quad 1], \quad (7)$$

$$H(x, u) = \begin{bmatrix} B_L u \\ h(C_L x_L, C_L [A_L x_L + B_L u], x_n) \end{bmatrix}. \quad (8)$$

Note that vector field $H(x(t), u(t))$ is not continuously differentiable in either $x(t)$ or $u(t)$. Also, observe that the imposed unity equilibrium transfer of system Σ_L does not limit the generality of the overall dynamics since the system function of Σ_H is able to accommodate any scaling of $y_L(t)$.

3. System analysis

In this section, we are chiefly concerned with the stationary behavior of the overall system for an input in the form of a continuous, monotone oscillating function of fixed amplitude, frequency, and phase. The structure of the overall model allows the behavior of $(u(t), y(t))$ to be composed from the behavior of $(u(t), y_L(t))$ and the behavior of $(y_L(t), y(t))$.

As far as the stationary behavior of $(u(t), y_L(t))$ is concerned, the asymptotic stability of linear system Σ_L is known to ensure that the application of an input $u(t)$ with aforementioned specifications is yielding a continuous, monotone oscillating $y_L(t)$ of fixed frequency, phase, and amplitude within a finite amount of time. The analysis into the stationary behavior of $(y_L(t), y(t))$ may therefore be limited to the case where $y_L(t)$ is a stationary oscillating function.

3.1. Stationarity

Let $y_L(t)$ be a stationary and monotone oscillating function of fixed amplitude and frequency, possibly with an offset. Under these conditions we may distinguish a $0 < T$, as well as two time instants t_1 and t_2 such that $t_1 \leq t_2 \leq t_1 + T$ and $y_{L,\min}$ and $y_{L,\max}$ represent the minimum and maximum value of $y_L(t)$ respectively)

$$y_L(t_1 + pT) = y_{L,\min} \wedge y_L(t_2 + pT) = y_{L,\max}, \quad p = 0, 1, \dots \quad (9)$$

Consequently, the first order time derivative of $y_L(t)$ is positive on open time interval $(t_1 + pT, t_2 + pT)$, and negative on $(t_2 + pT, t_1 + (p + 1)T)$.

Assume $t \in (t_1 + pT, t_2 + pT)$. Output $y(t)$ may then be regarded as a function $y^\uparrow(y_L(t)) = y(t)$ of linear system output $y_L(t)$ with a first order derivative with respect to y_L equal to

$$\frac{dy^\uparrow(y_L)}{dy_L} = -\alpha y^\uparrow(y_L) + \alpha f(y_L) + g(y_L). \quad (10)$$

Because of this differential equation's linear character as well as the continuity of $y(t)$ and $y_L(t)$ in t , we find that for $t_1 + pT \leq t \leq t_2 + pT$ output $y(t)$ may be determined as $y(t) = y^\uparrow(y_L(t); y(t_1 + pT))$ with $y^\uparrow(\cdot; y_0)$ the solution of (10) for initial value y_0 . Furthermore, the manner in which and the speed at which linear output $y_L(\cdot)$ reaches value $y_L(t)$ from $y_L(t_1 + pT)$ is irrelevant.

Next, let $t \in (t_2 + pT, t_1 + (p + 1)T)$. Output $y(t)$ is now interpreted as a function of $[-y_L(t)]$. The differential equation for $y^\uparrow([-y_L])$ is

$$\begin{aligned} \frac{dy^\uparrow([-y_L])}{d[-y_L]} &= -\alpha y^\uparrow([-y_L]) - \alpha f([-y_L]) - g([-y_L]). \end{aligned} \quad (11)$$

In view of the continuity in t of both $y(t)$ and $y_L(t)$, we conclude that for $t \in [t_2 + pT, t_1 + (p + 1)T]$ the value of output $y(t)$ may be evaluated as $y(t) = y^\uparrow([-y_L(t)]; y(t_2 + pT))$ with $y^\uparrow(\cdot; y_0)$ denoting the solution of (11) for initial value y_0 .

On the basis of these results we are able to derive iterative relations (with respect to p) for both $y(t_2 + pT)$ and $y(t_1 + pT)$. The output values $y_p^\uparrow \triangleq y(t_2 + pT)$ and $y_p^\downarrow \triangleq y(t_1 + pT)$ submit to the following time-invariant discrete-time systems with fixed driving terms:

$$\Sigma_H^\uparrow \triangleq \begin{cases} y_{p+1}^\uparrow = e^{-2\alpha[y_{L,\max} - y_{L,\min}]} y_p^\uparrow \\ \quad + \int_{y_{L,\min}}^{y_{L,\max}} e^{-\alpha[y_{L,\max} - s]} \{\alpha f(s) + g(s)\} ds \\ \quad - \int_{-y_{L,\max}}^{-y_{L,\min}} e^{-\alpha[y_{L,\max} - 2y_{L,\min} - s]} \{\alpha f(s) + g(s)\} ds \end{cases} \quad (12)$$

and

$$\Sigma_H^\downarrow \triangleq \begin{cases} y_{p+1}^\downarrow = e^{-2\alpha[y_{L,\max} - y_{L,\min}]} y_p^\downarrow \\ \quad + \int_{y_{L,\min}}^{y_{L,\max}} e^{-\alpha[2y_{L,\max} - y_{L,\min} - s]} \{\alpha f(s) + g(s)\} ds \\ \quad - \int_{-y_{L,\max}}^{-y_{L,\min}} e^{-\alpha[-y_{L,\min} - s]} \{\alpha f(s) + g(s)\} ds. \end{cases} \quad (13)$$

The fact that parameter α is positive is enough to ensure the asymptotic stability of the cross-coupled systems (12) and (13) since $0 < y_{L,\max} - y_{L,\min}$. Seeing that both y_p^\uparrow and y_p^\downarrow converge towards their respective equilibrium values after an arbitrary initial offset, we conclude that oscillating response $y(t)$ is asymptotically stationary.

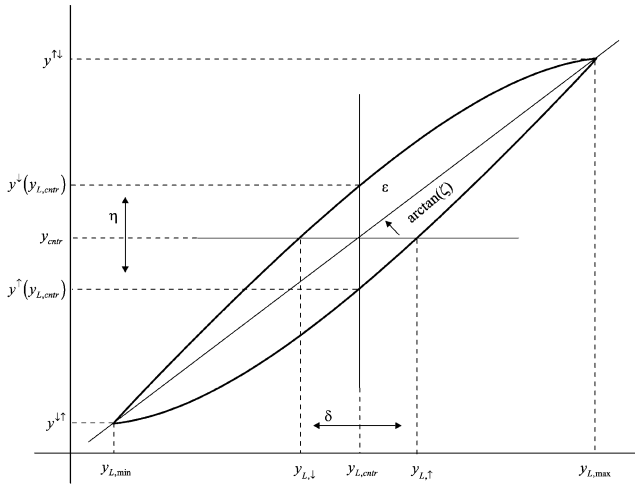


Fig. 1. Characteristic features of the stationary hysteresis loop.

3.2. The hysteresis loop

Consider an input/output pair $(y_L(t), y(t))$ of stationary oscillating functions. When $y_L(t)$ is plotted against $y(t)$, the result is a closed curve known as the *hysteresis loop* of the system, e.g. Fig. 1. Conditions 1 and 2 together with inequality (4) guarantee that this loop has a *counter-clockwise* orientation as time progresses. In addition, the piecewise monotony of the loop, i.e. $0 < \dot{y}_L(t)$ iff $0 < \dot{y}(t)$, is established when inequality (5) is adhered to (Coleman & Hodgdon, 1986).

The following *characteristic features* can be associated with the stationary hysteresis loop of system Σ_H : a *left turning point* $(y_{L,\min}, y^{\downarrow\uparrow})$, a *right turning point* $(y_{L,\max}, y^{\uparrow\downarrow})$, a *centre point* $(y_{L,\text{centr}}, y_{\text{centr}})$, a *horizontal aperture* δ , a *vertical aperture* η , a *slope* ζ , and a *hysteresis area* ϵ (see Fig. 1). It is evident from the graph in Fig. 1 that the coordinates of the centre point $(y_{L,\text{centr}}, y_{\text{centr}})$ may be determined as:

$$y_{L,\text{centr}} = \frac{1}{2}[y_{L,\min} + y_{L,\max}] \wedge y_{\text{centr}} = \frac{1}{2}[y^{\downarrow\uparrow} + y^{\uparrow\downarrow}] \quad (14)$$

and furthermore, that

$$\zeta \triangleq \frac{y^{\downarrow\uparrow} - y^{\uparrow\downarrow}}{y_{L,\max} - y_{L,\min}}, \quad (15)$$

$$\delta \triangleq y_{L,\uparrow} - y_{L,\downarrow}, \quad (16)$$

$$\eta \triangleq y^{\downarrow}(y_{L,\text{centr}}) - y^{\uparrow}(y_{L,\text{centr}}), \quad (17)$$

$$\epsilon \triangleq \int_{-y_{L,\max}}^{-y_{L,\min}} y^{\downarrow}([-y_L])d[-y_L] - \int_{y_{L,\min}}^{y_{L,\max}} y^{\uparrow}(y_L)dy_L. \quad (18)$$

Note that the coordinates $y^{\downarrow\uparrow}$ and $y^{\uparrow\downarrow}$ of the left and right turning point of the loop respectively, coincide with the equilibria of the discrete-time systems Σ_H^{\downarrow} and Σ_H^{\uparrow} respectively, and that for physical systems, the hysteresis area represents the amount of energy spent by the system (Coleman & Hodgdon, 1986). The result of the theorem

formulated below concerns the loop's centre point, and has a strong intuitive appeal.

Theorem 1. *The centre point of the hysteresis loop lies in the origin of $\mathbb{R} \times \mathbb{R}$ when $y_{L,\text{centr}} = 0$.*

Proof. It follows from the steady-state conditions for systems Σ_H^{\downarrow} and Σ_H^{\uparrow} that $(y_{L,\Delta} \triangleq y_{L,\max} - y_{L,\text{centr}} = y_{L,\text{centr}} - y_{L,\min})$

$$y^{\downarrow\uparrow} + y^{\uparrow\downarrow} = \frac{e^{-\alpha y_{L,\Delta}}}{1 - e^{-2\alpha y_{L,\Delta}}} \int_{-y_{L,\Delta}}^{y_{L,\Delta}} e^{zs} [\alpha f(s + y_{L,\text{centr}}) - \alpha$$

$$f(s - y_{L,\text{centr}}) + g(s + y_{L,\text{centr}}) - g(s - y_{L,\text{centr}})] ds.$$

Clearly, $y^{\downarrow\uparrow} + y^{\uparrow\downarrow}$ reduces to 0 when $y_{L,\text{centr}} = 0$. \square

The next theorem establishes a connection between functions $f(\cdot)$ and $g(\cdot)$ of the hysteresis dynamics and two of the five characteristic features of the stationary hysteresis loop.

Theorem 2. *For small values of the amplitude of $y_L(t)$, the centre point and the slope of the hysteresis loop may be approximated by $(y_{L,\text{centr}}, f(y_{L,\text{centr}}))$ and $\zeta = g(y_{L,\text{centr}})$ respectively.*

Proof. Consider, the first order Taylor approximations

$$f(s \pm y_{L,\text{centr}}) \approx \pm f(y_{L,\text{centr}}) + \frac{df(y_{L,\text{centr}})}{ds} s,$$

$$g(s \pm y_{L,\text{centr}}) \approx g(y_{L,\text{centr}}) \pm \frac{dg(y_{L,\text{centr}})}{ds} s,$$

$$se^{zs} \approx s.$$

Using these approximations for small $y_{L,\Delta}$, we find

$$\begin{aligned} y^{\downarrow\uparrow} + y^{\uparrow\downarrow} &\approx 2f(y_{L,\text{centr}}) \\ &+ 2 \frac{dg(y_{L,\text{centr}})}{ds} \frac{e^{-\alpha y_{L,\Delta}}}{1 - e^{-2\alpha y_{L,\Delta}}} \int_{-y_{L,\Delta}}^{y_{L,\Delta}} s ds \\ &= 2f(y_{L,\text{centr}}). \end{aligned}$$

The centre point is now easily determined. It follows from the steady-state conditions for systems Σ_H^{\downarrow} , and Σ_H^{\uparrow} that (use the Taylor approximations)

$$\begin{aligned} y^{\downarrow\uparrow} - y^{\uparrow\downarrow} &= \frac{e^{-\alpha y_{L,\Delta}}}{1 + e^{-2\alpha y_{L,\Delta}}} \int_{-y_{L,\Delta}}^{y_{L,\Delta}} e^{zs} [\alpha f(s + y_{L,\text{centr}}) + \alpha \\ &f(s - y_{L,\text{centr}}) + g(s + y_{L,\text{centr}}) \\ &+ g(s - y_{L,\text{centr}})] ds \\ &\approx \frac{e^{-\alpha y_{L,\Delta}}}{1 + e^{-2\alpha y_{L,\Delta}}} \int_{-y_{L,\Delta}}^{y_{L,\Delta}} 2\alpha \frac{df(y_{L,\text{centr}})}{ds} se^{zs} \\ &+ 2g(y_{L,\text{centr}})e^{zs} ds \end{aligned}$$

$$\begin{aligned} &\approx \frac{e^{-\alpha y_{L,\Delta}}}{1 + e^{-2\alpha y_{L,\Delta}}} \left\{ 2\alpha \frac{df(y_{L,\text{ctr}})}{ds} \int_{-y_{L,\Delta}}^{y_{L,\Delta}} s ds \right. \\ &\quad \left. + 2g(y_{L,\text{ctr}}) \frac{e^{2\alpha y_{L,\Delta}} - 1}{\alpha e^{\alpha y_{L,\Delta}}} \right\} \\ &= 4y_{L,\Delta} g(y_{L,\text{ctr}}) \frac{1 - e^{-2\alpha y_{L,\Delta}}}{2\alpha y_{L,\Delta}} \\ &\quad \frac{1}{1 + e^{-2\alpha y_{L,\Delta}}} \approx 2y_{L,\Delta} g(y_{L,\text{ctr}}). \end{aligned}$$

From this result follows the expression for ζ . \square

3.3. Overall input/output analysis

For input signals in the form of a continuous, monotone oscillating function of fixed amplitude, phase, and sufficiently low driving frequency, the asymptotically stable linear dynamics act as a unity gain, i.e. $y_L(t) = u(t)$. As a matter of consequence, the input/output graph between $u(t)$ and $y(t)$ is coincident with the hysteresis loop between $y_L(t)$ and $y(t)$ and can, therefore, be attributed with a well-defined centre point, slope, horizontal and vertical aperture, as well as a hysteresis area.

When input $u(t)$ is a continuous, high-frequency monotone oscillating function of fixed amplitude and phase, linear output $y_L(t)$ converges towards a stationary response. The amplitude and the phase angle of $y_L(t)$ are now, however, dependent upon the driving frequency of $u(t)$. Although neither the frequency nor the phase angle of $y_L(t)$ have any effect on the hysteresis loop between $y_L(t)$ and $y(t)$, the phase shift between $u(t)$ and $y_L(t)$ does indicate that the loop between $u(t)$ and $y(t)$ is no longer identical to the loop between $y_L(t)$ and $y(t)$. Indeed, the aforementioned phase shift manifests itself as a distortion (with respect to the loop in the y_L/y plane) in the loop between $u(t)$ and $y(t)$.

4. System identification

The problem of devising a set of experiments that will allow the complete identification of state-space realization Σ_O as presented in Section 2 is the topic of research in this section. The results of the previous section tell us that the dynamic effect between $u(t)$ and $y(t)$ is predominantly hysteretic in nature for low-frequency sinusoidal inputs, and that it is a mixture of the linear and the hysteresis dynamic effects for high-frequency sinusoidal inputs. It was also demonstrated that certain characteristic features attributed to the stationary hysteresis loop have a strong relation to the functions featuring in the hysteresis dynamics (Theorem 2). This is especially interesting when we recall that the loop's characteristic features are empirically determinable.

4.1. Model selection

In Holman, Laman, Scholte, Heerens, and Tuinstra (1996), position measurements have been presented for a translation stage driven by piezoelectric actuators. The measured hysteresis loop between a low-frequency voltage signal (input) and the corresponding position signal (output) is similar in shape to the simulated hysteresis loops reported upon in Coleman and Hodgdon (1986). This simulated hysteresis loop features a function $f(v)$ that is proportional in v , and a function $g(v)$ that is constant in v . In view of these considerations, we adopt here the following choice for functions $f(\cdot)$ and $g(\cdot)$ ($0 < s_{\max}$):

$$f(s) = \begin{cases} as_{\max} & \text{if } s_{\max} < s, \\ as & \text{if } -s_{\max} \leq s \leq s_{\max}, \\ as_{\min} & \text{if } s < -s_{\max} \end{cases} \quad (19)$$

and

$$g(s) = \begin{cases} 0 & \text{if } s_{\max} < s, \\ b & \text{if } -s_{\max} \leq s \leq s_{\max}, \\ 0 & \text{if } s < -s_{\max} \end{cases} \quad (20)$$

with $0 < a$ and $0 < b$. Clearly, functions $f(\cdot)$ and $g(\cdot)$ agree with conditions 1 and 2 presented earlier. Furthermore, functions $f(\cdot)$ and $g(\cdot)$ are compliant with inequalities (4) and (5) for a and b such that $\frac{1}{2}a \leq b < a$.

An example of a hysteresis loop generated with the hysteresis model based on these functions is available in Fig. 2. The aforementioned measurement data (Holman, Laman, Scholte, Heerens, and Tuinstra 1996), and the simulation results suggest that we may assume the values of variable $y_L(t)$ to lie within $(-s_{\max}, s_{\max})$ from hereon.

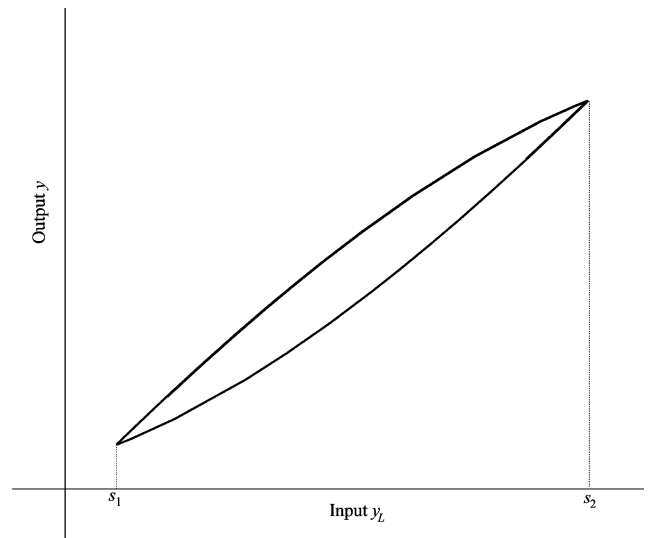


Fig. 2. Simulated stationary hysteresis loop with $-s_{\max} \ll s_1 \leq y_L \leq s_2 \ll s_{\max}$.

4.2. Hysteresis identification

The application of a low-frequency sinusoidal signal $u(t) = \bar{u} + \mathcal{A} \sin[\omega t]$ as input to device dynamics (6) is known to yield a hysteresis loop in the u/y plane for all practical purposes. The characteristic features of the hysteresis loop can all be determined experimentally. For their theoretical evaluation, we rely on the following theorem.

Theorem 3. *Let the sinusoidal input signal $u(t) = \bar{u} + \mathcal{A} \sin[\omega t]$ for the overall system dynamics be such that $y_L(t) = u(t)$. The centre point of the hysteresis loop in the u/y plane is then $(\bar{u}, a\bar{u})$. The remaining characteristic features of the hysteresis loop can be determined as*

$$\zeta = a + \frac{b - a}{\alpha} \frac{1 - e^{-2\alpha\mathcal{A}}}{\mathcal{A}(1 + e^{-2\alpha\mathcal{A}})} \approx b, \tag{21}$$

$$\delta \approx 2 \frac{a - b}{\alpha} \frac{(1 - e^{-\alpha\mathcal{A}})^2}{a(1 - e^{-\alpha\mathcal{A}})^2 + 2be^{-\alpha\mathcal{A}}} \approx \alpha \left(\frac{a}{b} - 1 \right) \mathcal{A}^2, \tag{22}$$

$$\eta = 2 \frac{a - b}{\alpha} \frac{(1 - e^{-\alpha\mathcal{A}})^2}{1 + e^{-2\alpha\mathcal{A}}} \approx \alpha(a - b)\mathcal{A}^2, \tag{23}$$

$$\varepsilon = 4 \frac{a - b}{\alpha} \left\{ \mathcal{A} - \frac{1}{\alpha} \frac{1 - e^{-2\alpha\mathcal{A}}}{1 + e^{-2\alpha\mathcal{A}}} \right\} \approx \frac{4}{3} (a - b) \alpha \mathcal{A}^3. \tag{24}$$

The approximations are valid for $\alpha\mathcal{A} \ll 1$.

Proof. The right and left turning points of the hysteresis loop between input $u(t)$ and output $y(t)$ represent the equilibrium points of systems Σ_H^\downarrow and Σ_H^\uparrow , respectively and, as such, are determined as

$$y^{\uparrow\downarrow} = ay_{L,\max} + \frac{b - a}{\alpha} \frac{1 - e^{-2\alpha\mathcal{A}}}{1 + e^{-2\alpha\mathcal{A}}},$$

$$y^{\downarrow\uparrow} = ay_{L,\min} - \frac{b - a}{\alpha} \frac{1 - e^{-2\alpha\mathcal{A}}}{1 + e^{-2\alpha\mathcal{A}}}.$$

From these expressions we find that the centre point of the hysteresis loop is positioned at $(\bar{u}, a\bar{u})$. The loop's slope ζ can be determined as

$$\zeta = a + 2(a - b) \frac{1 - e^{-2\alpha\mathcal{A}}}{-2\alpha\mathcal{A}} \frac{1}{1 + e^{-2\alpha\mathcal{A}}} \approx a - (a - b) = b$$

for sufficiently small amplitudes \mathcal{A} . Evaluation of δ in closed form requires the inverse of the hysteresis model. The expression for δ presented in this theorem relies, therefore, on the approximation $1 - e^{-(1/2)\alpha\delta} \approx \frac{1}{2}\alpha\delta$,

which is valid for small values of $\alpha\delta$. Using this approximation we obtain

$$\begin{aligned} \delta &\approx 2 \frac{a - b}{\alpha} \frac{\{1 - e^{-\alpha\mathcal{A}}\}^2}{a\{1 - e^{-\alpha\mathcal{A}}\}^2 + 2be^{-\alpha\mathcal{A}}} \\ &= 2 \left\{ \frac{1 - e^{-\alpha\mathcal{A}}}{-\alpha\mathcal{A}} \right\}^2 \frac{\alpha\mathcal{A}^2(a - b)}{a(1 - e^{-\alpha\mathcal{A}})^2 + 2be^{-\alpha\mathcal{A}}} \\ &\approx \alpha \left(\frac{a}{b} - 1 \right) \mathcal{A}^2 \end{aligned}$$

for small enough values of $\alpha\mathcal{A}$. Vertical aperture η represents the distance between $(y_{L,\text{entr}}, y^\uparrow(y_{L,\text{entr}}))$ and $(y_{L,\text{entr}}, y^\downarrow(y_{L,\text{entr}}))$. For $\alpha\mathcal{A}$ sufficiently small, we obtain the approximation

$$\eta = 2\alpha\mathcal{A}^2(a - b) \left\{ \frac{1 - e^{-\alpha\mathcal{A}}}{-\alpha\mathcal{A}} \right\}^2 \frac{1}{1 + e^{-2\alpha\mathcal{A}}} \approx \alpha(a - b)\mathcal{A}^2.$$

Finally, the two integrals in expression (18) for hysteresis area ε are readily solved. The small amplitude approximation presented is obtained by using the third order Taylor approximation for the non-linear expression in $\alpha\mathcal{A}$. \square

According to Theorem 3, parameter a of the hysteresis dynamics determines the variation in the loop's centre point when input offset \bar{u} is altered. Furthermore, parameter b coincides with the loop's slope when amplitude \mathcal{A} of the input signal is sufficiently small. The remaining unknown parameter of the hysteresis model, i.e. parameter α , may subsequently be derived from the variation in the hysteresis area ε due to changes in input amplitude \mathcal{A} .

An important aspect of the results of Theorem 3 is that every characteristic feature but the centre point is invariant with respect to offset \bar{u} . It would, therefore, appear that the *shape* of the hysteresis loop is preserved under changes in \bar{u} . Confirmation of the truth of this suggestion lies in the fact that the dynamic behaviour between $[y_L(t) - \bar{u}]$ and $[y(t) - a\bar{u}]$ submits to the same differential equation that governs the pair $(y_L(t), y(t))$:

$$\begin{aligned} \frac{d[y(t) - a\bar{u}]}{dt} &= -\alpha[y(t) - a\bar{u}] \left| \frac{d[y_L(t) - \bar{u}]}{dt} \right| \\ &\quad + \alpha a[y_L(t) - \bar{u}] \left| \frac{d[y_L(t) - \bar{u}]}{dt} \right| \\ &\quad + b \frac{d[y_L(t) - \bar{u}]}{dt}. \end{aligned}$$

4.3. Linear system identification

Consider the application of $u(t) = \bar{u} + \mathcal{A} \sin[\omega t]$, ω arbitrary, as input to the overall system dynamics. The stationary linear output $y_L(t)$ associated with $u(t)$ is $y_L(t) = \bar{u} + \mathbf{h}(\omega)\mathcal{A} \sin[\omega t + \varphi]$ for $\mathbf{h}(\omega) \triangleq |\mathbf{H}(j\omega)|$, and

$\mathbf{H}(s)$ the Laplace domain transfer function of linear system Σ_L . The relations between $y_{\max} = y^{\uparrow\downarrow}$ and $y_{\min} = y^{\downarrow\uparrow}$ on the one hand and $y_{L,\max}$ and $y_{L,\min}$ on the other hand can be combined to yield

$$y_{\max} - y_{\min} = 2a\mathbf{h}(\omega)\mathcal{A} + 2\frac{b-a}{\alpha} \frac{1 - e^{-2\alpha\mathcal{A}\mathbf{h}(\omega)}}{1 + e^{-2\alpha\mathcal{A}\mathbf{h}(\omega)}}. \quad (25)$$

In principle, this relation can be exploited for the numerical evaluation of *magnitude response* $\mathbf{h}(\omega)$ at different values of driving frequency ω . Unfortunately, a closed form expression for the inverse, with respect to $\mathbf{h}(\omega)$, of the right hand side expression is not readily available. We therefore propose the following approximation to the non-linearity in $\alpha\mathcal{A}\mathbf{h}(\omega)$, i.e.

$$\frac{1 - e^{-2\alpha\mathcal{A}\mathbf{h}(\omega)}}{1 + e^{-2\alpha\mathcal{A}\mathbf{h}(\omega)}} \approx \alpha\mathcal{A}\mathbf{h}(\omega). \quad (26)$$

Based on this approximation, relationship (25) boils down to

$$\mathbf{h}(\omega) = \frac{y_{\max} - y_{\min}}{2b\mathcal{A}}. \quad (27)$$

This result can be used for evaluation of transfer function $\mathbf{H}(s)$ on the basis of experimental data once parameter b has been deduced from the hysteresis identification experiments.

5. Example

The 2D translation stage with integrated capacitive sensors and piezoelectric actuators as presented in Holman, Laman, Scholte, Heerens, and Tuinstra (1996) is an example of a system with both linear and hysteretic dynamic behaviour. This stage is used for the purpose of sample positioning in the so-called scanning tunnelling microscope. The operating range of the two identical piezoelectric actuators is 1000 V (−750, +250). The average sensitivity of each piezoelectric actuator is 10 nm/V in unloaded condition. All experiments will be performed from within MATLAB^(R) using a dSPACE^(R) DSP system. The sampling frequency is fixed at 10 kHz.

5.1. System definition

The symmetrical design of the 2D translation stage guarantees two uncoupled directions of motion with identical dynamic behaviour. Consequently, we only consider the dynamic behaviour of the stage in one direction of motion. The stage without sensors and actuators is, essentially, a damped mass-spring-system. A detailed modelling effort for mechanical systems driven by piezoelectric actuators is outside the scope of this paper. However, it has been demonstrated that for sufficiently

small input signals of arbitrary frequency, such a system is adequately represented by a linear dynamic system in series with a hysteresis system in the manner considered in this paper (Koning de, Adriaens, & Banning, 1998).

We attempt to fit overall system Σ_O to the linear dynamic and hysteretic behaviour of the stage. The linear dynamics Σ_L describe the predominantly linear dynamic behaviour of the stage. The second order linear equation of motion for a damped mass-spring-system is

$$\ddot{y}_L(t) + c\dot{y}_L(t) + ky_L(t) = \beta u(t). \quad (28)$$

The normalized canonical controllability state-space realization for this equation of motion features only two independent parameters ($0 < k, 0 < c$) and is of the form

$$\Sigma_L = \begin{cases} \frac{dx_L(t)}{dt} = \begin{bmatrix} 0 & 1 \\ -k & -c \end{bmatrix} x_L(t) + \begin{bmatrix} 0 \\ k \end{bmatrix} u(t), \\ y_L(t) = [1 \quad 0] x_L(t). \end{cases} \quad (29)$$

Functions $f(\cdot)$ and $g(\cdot)$ as specified in (19) and (20) respectively, will be used to form the differential model of hysteresis Σ_H , i.e.

$$\Sigma_H = \left\{ \frac{dw(t)}{dt} = -\alpha w(t)|\dot{v}(t)| + \alpha av(t)|\dot{v}(t)| + b\dot{v}(t). \right. \quad (30)$$

The overall dynamics with state-space realization Σ_O are composed in the manner described in Section 2.

5.2. Hysteresis identification experiments

Application of a voltage signal $u(t) = \bar{u} + \mathcal{A} \sin[\omega t]$ (assume a low-frequency ω) to the piezos driving the translation stage, is yielding a stationary system response $y(t)$ within a finite amount of time. For the purpose of determining parameter a , we execute a series of experiments in which only offset \bar{u} is varied. For every measured stationary hysteresis loop, the centre point is evaluated. The results of this experiment can be seen in Fig. 3; the open circlets represent empirically obtained centre points while the solid line represents a first order least-squares approximation.

When amplitude \mathcal{A} of the sinusoidal voltage signal is small enough, the slope of the hysteresis loop is equal to b . Another sequence of experiments is therefore executed in which not \bar{u} , but amplitude \mathcal{A} is varied in the appropriate range. In Fig. 4, the experimental slope values, i.e. the open circlets, have been set out against amplitude \mathcal{A} ; the solid line represents their mean value.

With the evaluation of a and b complete, parameter α can be determined from the fit of expression (24) to a series of experimentally determined values for ε (voltage

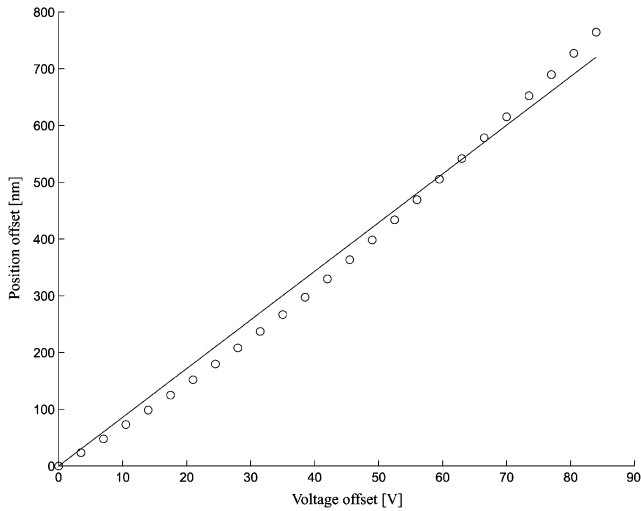


Fig. 3. Measured centre point of a stationary hysteresis loop versus the applied voltage offset, together with the best linear approximation.

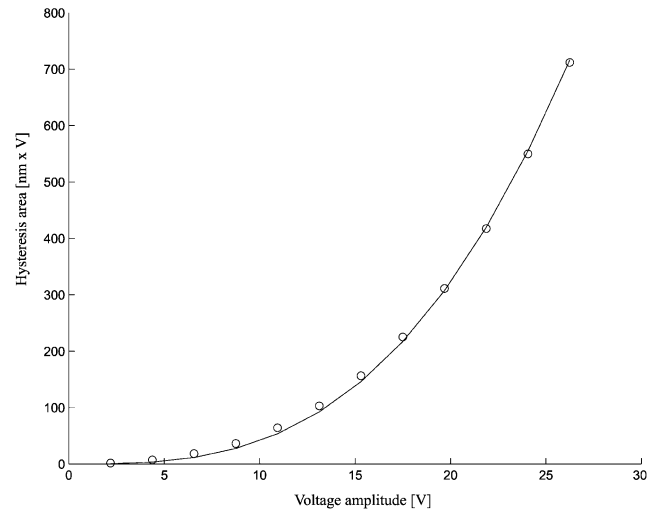


Fig. 5. Measured hysteresis area of a stationary hysteresis loop versus the applied voltage amplitude, and the optimal theoretical fit.

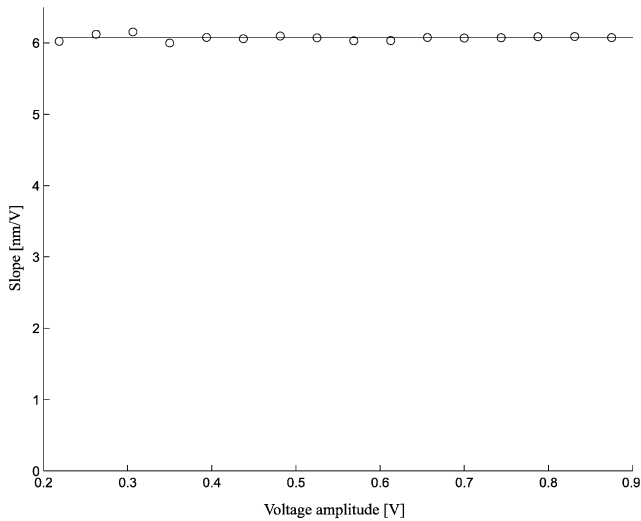


Fig. 4. Measured slope of a stationary hysteresis loop versus the applied voltage amplitude, and the constant average value.

Table 1

Parameters of the differential model of hysteresis

a (nm V ⁻¹)	b (nm V ⁻¹)	α (V ⁻¹)
8.58	6.07	0.0123

amplitude \mathcal{A} is changing; \bar{u} is fixed arbitrarily and ω is sufficiently low). In Fig. 5, the hysteresis area measurements (the open circlets) are displayed against \mathcal{A} together with the least-squares fit for function (24) (the solid graph). The values of parameters a , b , and α determined in these fashions, are available in Table 1.

5.3. Linear system identification experiments

For the identification of the parameters of the linear system dynamics, we rely on experiments in which the driving frequency of input signal $u(t) = \bar{u} + \mathcal{A} \sin[\omega t]$ is not fixed. While maintaining a constant small voltage amplitude \mathcal{A} we allow frequency ω to vary from experiment to experiment. Through exploitation of relation (27)

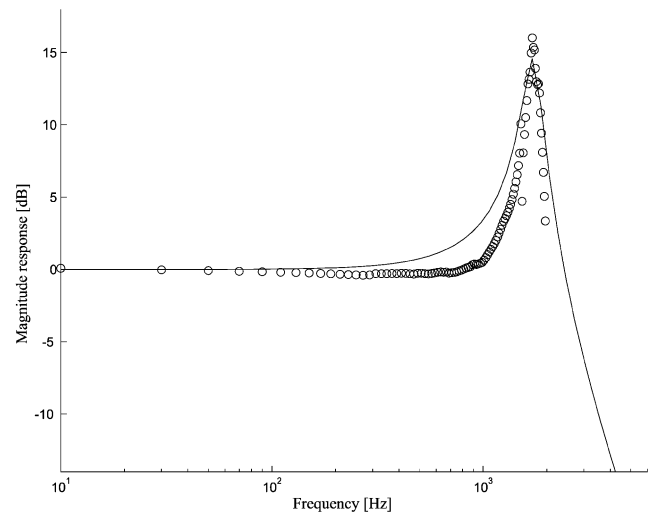


Fig. 6. Measured magnitude response versus frequency, together with a fit for a second order dynamic system.

we can effectively measure the magnitude response of the linear dynamics.

In Fig. 6, the open circlets represent the measured values of $\mathbf{h}(\omega)$ for different values of driving frequency ω . The solid line in the graph is the selected fit for a second order system with state-space realization (29). It is obvious from the graphs in this figure that our model

Table 2
State-space realization for the normalized linear dynamics

Matrix A_L	Matrix B_L	Matrix C_L
$\begin{bmatrix} 0 & 1 \\ -1.17 \times 10^8 & -2.03 \times 10^3 \end{bmatrix}$	$\begin{bmatrix} 0 \\ 1.17 \times 10^8 \end{bmatrix}$	$[1 \ 0]$

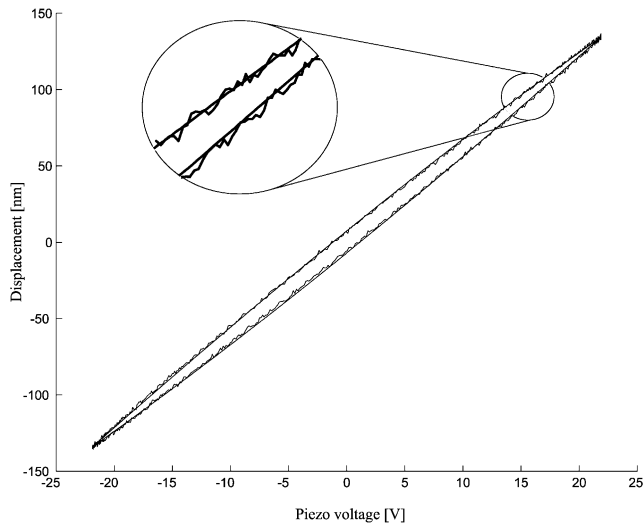


Fig. 7. Measured and simulated, low-frequency stationary hysteresis loops.

adequately captures the dominant resonance peak of the stage dynamics. The values of the identified matrices of the normalized linear system dynamics are available in Table 2.

With the state-space model completely known, we are able to perform simulations in order to verify the correctness of the model. A typical pair of measured and simulated stationary hysteresis loops for a low-frequency (2 Hz) sinusoidal voltage signal, is displayed in Fig. 7. Bearing in mind that the simulation model does not allow for measurement noise, we conclude that our identification effort is successful in view of the admirable reproduction of the dynamic stage behaviour by our model.

6. Conclusions

In this paper, we focus on the twin issues of modelling and identification for a dynamic system affected by hysteresis. The purpose of the modelling and identification effort is to obtain a system amenable to model-based state-space control methods, hence the choice for the series connection of a differential model of hysteresis (on

the output side) and a linear time-invariant dynamic system, as the overall dynamic model.

The overall dynamic relation between system input and system output is, in general, compounded from linear and hysteretic dynamic effects. Of the findings of the dynamic system analysis, three results stand out in particular. The first of these results demonstrates that the linear dynamic effect can be neutralized via a suitably chosen input signal without affecting the hysteretic dynamic effect. The second of the results referred to states that the linear and dynamic effects can be peeled apart, again, for a certain class of input signals. The last of the three results draws attention to the fact that the dynamic effect between input and output can be conveniently expressed in the input/output plane.

The results of the dynamic system analysis can be shown to produce workable identification recipes, once a particular hysteresis model is adopted. These recipes allow the complete identification of the system's state-space realization and rely on the use of stationary sinusoidal input signals. Finally, the developed identification tools are used successfully for the purpose of fitting a dynamic model on a high-precision translation stage under the influence of hysteresis.

Acknowledgements

This research is supported by the Dutch Technology Foundation (STW).

References

- Adriaens, J. M. T. A., de Koning, W. L., & Banning, R. (1999). Feedback-linearization control of a piezo-actuated positioning mechanism. *Proceedings of the fifth European control conference*, CD-ROM, paper f0671.
- Banning, R., de Koning, W. L., & Adriaens, J. M. T. A. (1999). Discrete-time tracking control for hysteretic systems. *Proceedings of the fifth European control conference*, CD-ROM, paper f0564.
- Coleman, B. D., & Hodgdon, M. L. (1986). A constitutive relation for rate-independent hysteresis in ferromagnetically soft materials. *International Journal of Engineering Science*, 24(6), 897–919.
- Ge, P., & Jouaneh, M. (1996). Tracking control of a piezoceramic actuator. *IEEE Transactions on Control Systems Technology*, 4(3), 1–7.
- Goldfarb, M., & Celanovic, N. (1997). Modeling piezoelectric stack actuators for control of micromanipulation. *IEEE Transactions on Control Systems Technology*, 17(3) 69–79.
- Hodgdon, M. L. (1988). Applications of a theory of ferromagnetic hysteresis. *IEEE Transactions on Magnetics*, 24(1), 218–221.
- Holman, A. D., Laman, C. D., Scholte, P. M. L. O., Heerens, W. Chr., & Tuinstra, F. (1996). A calibrated scanning tunneling microscope equipped with capacitive sensors. *Review of Scientific Instruments*, 67(5), 2274–2280.
- Koning de, W. L., Adriaens, J. M. T. A., & Banning, R. (1998). Physical modeling of piezoelectric actuators for control purposes. *Proceedings of the IFAC workshop on motion control*, Grenoble, France (pp. 37–42).

Krasnoselskii, M. A., & Pokrovskii, A. V. (1989). *Systems with hysteresis*. Berlin: Springer.

Tao, G., & Kokotovic, P. V. (1996). *Adaptive control of systems with actuator and sensor nonlinearities*. New York: Wiley.

Visintin, A. (1994). *Differential models of hysteresis*. Berlin: Springer.



Reinder Banning was born in 1966 in Leeuwarden, The Netherlands. In 1989 he obtained the M.Sc. degree in Applied Mathematics from the University of Twente, The Netherlands. At the end of a research assistantship at Strathclyde University, Scotland, he got his Ph.D. degree in Electronic & Electric Engineering in 1993. Since then, he has been an Assistant Professor in systems and control at the Department of Applied Physics, Delft University of Technology, The Netherlands.

His research interests include optimal control, non-linear systems and control, nanometer positioning, and stochastic systems.



Willem de Koning was born in 1944 in Leiden, The Netherlands. He received the M.Sc. and Ph.D. degrees in Electrical Engineering from the Delft University of Technology, The Netherlands in 1975 and 1984, respectively. From 1969 to 1975 he was a Research Engineer of Power Electronics and Control in the Department of Electrical Engineering, Delft University of Technology. From 1975 to 1987 he was an Assistant Professor of Process Dynamics and Control in the Department of Applied

Physics. Since 1987 he is an Associate professor of Mathematical System Theory in the Department of Information Technology and Systems. He has held a visiting position at the Florida Institute of Technology, Melbourne. His research interests include control of distributed-parameter systems, reduced-order control, adaptive predictive control, digital control, and applications.



Han Adriaens was born in 1972 in Geldrop, The Netherlands. In 1996 he received the M.Sc. degree in Mechanical Engineering from the Eindhoven University of Technology and in 2000 he received the Ph.D. degree in Applied Mathematics from the Delft University of Technology. Currently he works at ASML, Veldhoven, The Netherlands, where machines for semiconductor manufacturing are developed and produced. His main research interest is in applied mathematics, with

a focus on non-linear systems and control and on measurement systems.



Richard Koops was born in 1961 in Groningen, The Netherlands. In 1986 he obtained the M.Sc. degree in Experimental Physics at the University of Groningen. As a result of a Ph.D. project in the field of Scanning Probe Microscopy at the same university he obtained his degree in 1992. After various postdoc positions at the Delft University of Technology he is now a research scientist at the NMI-VSL, the Dutch Metrology Institute, working in the field of nanometrology and primary length standards.